transmission curves, detector efficiencies, mirror reflectivities, etc. This database is useful also in the preparation of the observations for estimating the exposure times.

Figure 1 shows the results of the application of these techniques to the imaging of a radio galaxy, showing how well the ionized gas can be separated from the stellar component in a case where the two have a clearly different structure.

Velocity and Velocity Dispersion Fields of NGC 6684: An SB0 Galaxy with a Ring

D. BETTONI, Astronomical Observatory of Padua, Italy
G. GALLETTA, Astronomy Department, University of Padua, Italy

1. Observations

NGC 6684 is a southern S0 galaxy of magnitude B = 11.35 showing a bright bar aligned about 20° from the minor axis of the disk and encircled by an elongated luminous ring (b/a = 0.77). This galaxy has been observed within a programme of study of stellar motions in barred galaxies, a subject which in the recent years has been analysed by many theoretical works but that has been studied observationally only by few authors. Among the galaxies for which the whole stellar velocity field is known, the velocity dispersion field has been studied only for NGC 936 (Kormendy, 1984).

NGC 6684 was observed in May 1983 and March 1984 at the 3.6-m telescope of the European Southern Observatory at La Silla, Chile. The spectra were taken using the Cassegrain Boller and Chivens spectrograph plus a 3-stage EMI image tube and setting the slit at four different position angles corresponding to the apparent major and minor axes of the disk, the bar major axis and to a P.A. at 45° from the major axis. The spectra of some early K-type giant stars were recorded each night, for use in the reductions as template stars of zero velocity dispersion. The exposure times were ranging from 30 to 55 minutes. The slit was set to a width of 1.5 arcseconds on the sky and to a length of 1.9 arcminutes. The plate scale along the slit image was 38.5 arcsec mm^{-1}, and the dispersion was 39 Å/mm.

The spectroscopic observations of the galaxy were associated to a morphological study based on two 15-minute V frames taken with the 320 × 512 RCA CCD of the 1.5-m Danish telescope on the night of May 6/7, 1986 and on the analysis of the galaxy images on ESO (B) and ESO/SRC (J) charts. In the following we describe some of the more interesting results arising from our observations.

Data Reduction and Analysis

All the spectra have been digitized with the ESO PDS microdensitometer using a 12.5 × 50 μ slit and considering a wavelength interval of 3800–4500 Å. No emission lines were detected in the spectra, but CaII H and K absorption and G-band are well defined. All the PDS images were calibrated in intensity and wavelength and sky subtracted using the ESO-IHAP procedure at the Padova HP computer centre. The resulting images were continuum flattened and analysed with the Fourier Quotient Technique described in Bertola et al. (1984), giving simultaneously the radial velocity, the velocity dispersion and the line-strength parameter for each scan line of each spectrum. The curvature of the spectral lines has been measured from a full slit comparison spectrum by measuring with the Grant 2 coordinate machine of ESO the position of 12 spectral lines. It has been found quite negligible, producing a shift lower than

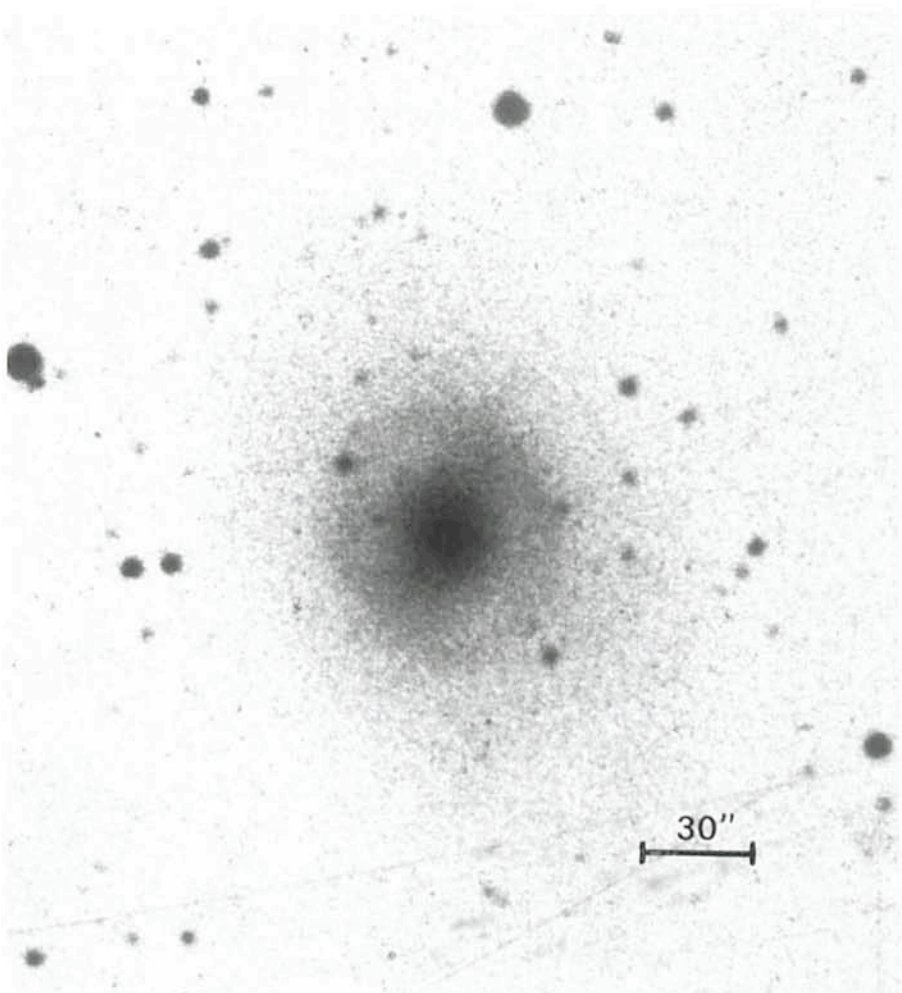

Figure 1: *Image of NGC 6684 from ESO (B) chart.*

TABLE 1: *Intrinsic shape of the single component of NGC 6684, as deduced from the isophote flattening and orientation. The lines of the nodes have been assumed at $\Phi = 42°$, P.A. of the disk, and the inclination of the galactic plane is $i = 48°.4$.*

	OBSERVED PARAMETERS			INTRINSIC PARAMETERS				PROJECTED VALUES	
component	q_o	$(\Phi - \Phi_n)_o$	r	δ	q	p	R	q_c	$(\Phi - \Phi_n)_c$
disk	0.69 ± 0.03	0° ± 5°	–	0°	0.250	1.000*	–	–	–
bar	0.60 0.04	108° 2°	30″	102°	0.443	0.454	44″	0.600	108.0
ring	0.77 0.01	174° 2°	37″	102°	0.000*	0.847	54″	0.766	172.7
bulge	0.83 0.03	166° 8°	10″	159°	0.817	0.824	11″	0.830	166.0

* values assumed.

10 km/s for points having $r \leq 30''$ from the nucleus. All the velocities have been corrected to the Sun. The mean velocity and velocity dispersion of the nucleus are found to be $V_o = 866 \pm 22$ km/s and $\bar{\sigma}_o = 93 \pm 12$ km/s respectively. The mean nuclear velocity is slightly higher than previous determinations for the redshift of NGC 6684: 812 ± 30 km/s (Corwin and Emerson 1982) and 823 km/s (de Vaucouleurs et al. 1976, RC 2).

The above data allow us to produce maps of the velocity dispersion and velocity fields. These are reproduced on the same scale in Figures 2 and 3 respectively. To analyse the large-scale kinematical features of the galaxy, all the data have been smoothed with a gaussian weighting function (FWHM = 4″) and rebinned at 3″ interval before being plotted in the maps. The velocities are scaled to the systemic velocity and lines of equal velocity and velocity dispersion have been drawn interpolating by eye from the observed values. In the case of the velocity field, the curvature of the outer lines has been assumed from the estimate of the P.A. corresponding fo the maximum velocity gradient made in the next paragraph. For the velocity dispersion we tried to show the elongation of the equivelocity lines due to the presence of the bar with respect to the more symmetric structure of the bulge + disk component.

The shape and the orientation of the four galaxy components (disk, ring, bar and bulge) has been measured on the CCD frames and on the ESO/SRC (J) and ESO (B) charts (Fig. 1), producing the mean values listed in the three first colums of the Table 1. They are, for each component: the observed axial ratio $\underline{q}_o$, the position angle φ of the major axis (referred to that of the disk) and its extension r. Analysing the light distribution, we observed the presence of a progressive shift of the bar isophote to the NW, indicating a displacement of the bar centre with respect to the galaxy nucleus. The amount of this displacement has been evaluated as 2″ to the NW. The mean values listed in Table 1 were analysed in order to deduce the intrinsic shape of the light distribution. Since each one of the isophotes could be considered as the projection of an ellipsoidal shell with intrinsic axial ratios $\underline{q} = c/a$, $\underline{p} = b/a$ ($a > b > c$), it is possible in principle to deduce the values of $\underline{q}$ and $\underline{p}$ by deprojecting the observed ellipticities and position angles. This is a simple geometrical problem which allows only one solution, providing that the orientation angles of each ellipsoid with respect to the line of sight are de-

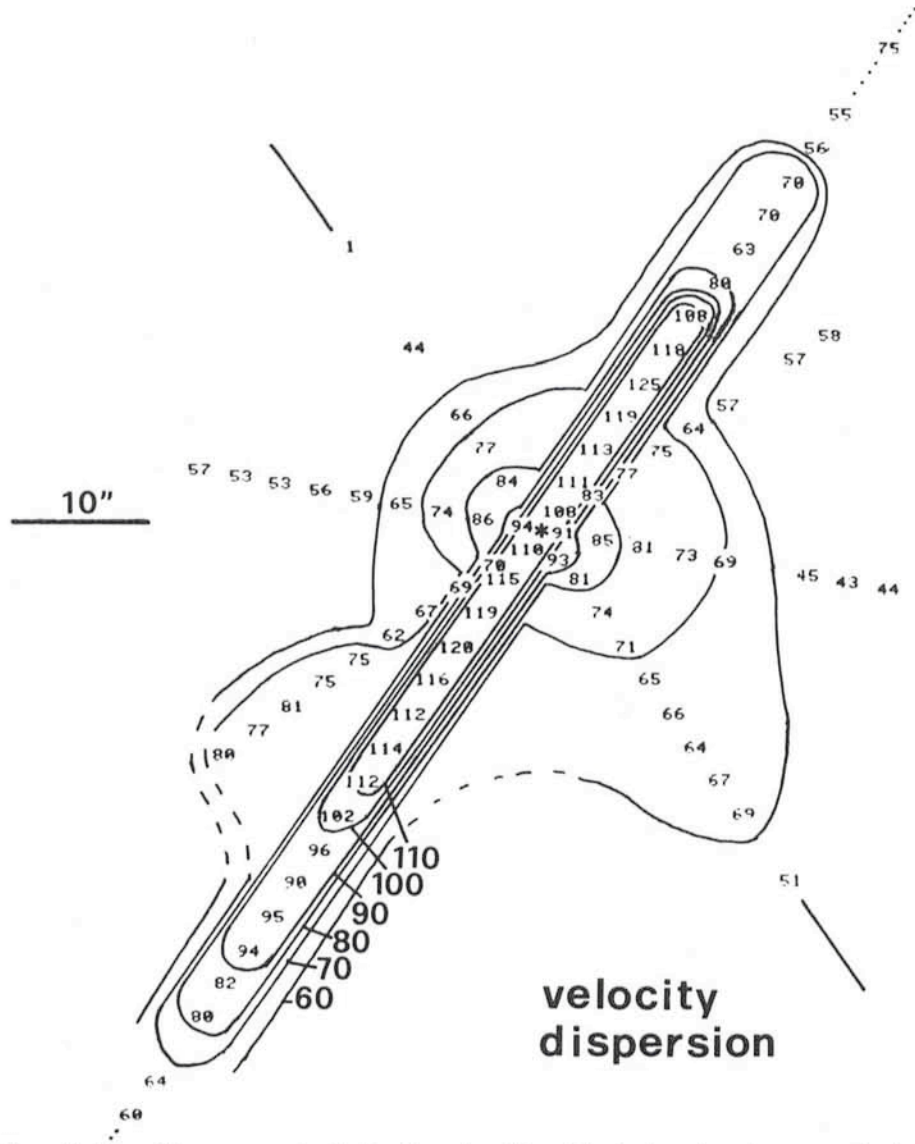

Figure 2: *Map of the measured velocity dispersion. The original values have been smoothed with a gaussian weighing function (FWHM = 4 arcsec) and rebinned each 3 arcsec before being plotted in the maps. Lines of equal velocity dispersion have been drawn interpolating by eye from the observed values and taking into account the geometry of the system (bar+disk). An asterisk represents the position of the nucleus. The direction of the disk's major axis (full line), that of the bar (dotted line) and the scale of the image are shown.*

fined (see Williams 1981, and Galletta 1983). The only exception to the uniqueness of the solution is the indeterminate case where the observed P.A. coincides with the line of the nodes. The analysis is composed by three main steps: First, from the apparent flattening of the disk, assuming an intrinsic axial ratio of 0.25 (Sandage et al. 1970), we deduce its inclination with respect to the plane of the sky and the P.A. φ_n of the line of the nodes. This produces the values $i = 48.4°$ and $\varphi_n = 42°$ respectively. Second, by means of these values we deproject on the plane of the galaxy all the distances r and the P.A. φ observed on the sky and we define, as a first approximation, the true extention R of each component of NGC 6684 and the angle δ formed by its major axis with the line of the nodes. Finally, synthetic isophotes are produced with different values of $\underline{q}$ and $\underline{p}$ and the resulting flattenings and P.A. are compared with the observed values of Table 1, until a satisfying agreement within the measuring errors is found. The values so obtained are indicated in Table 1, columns from 5 to 7, and the ranges of acceptable solutions are shown in Figure 4.

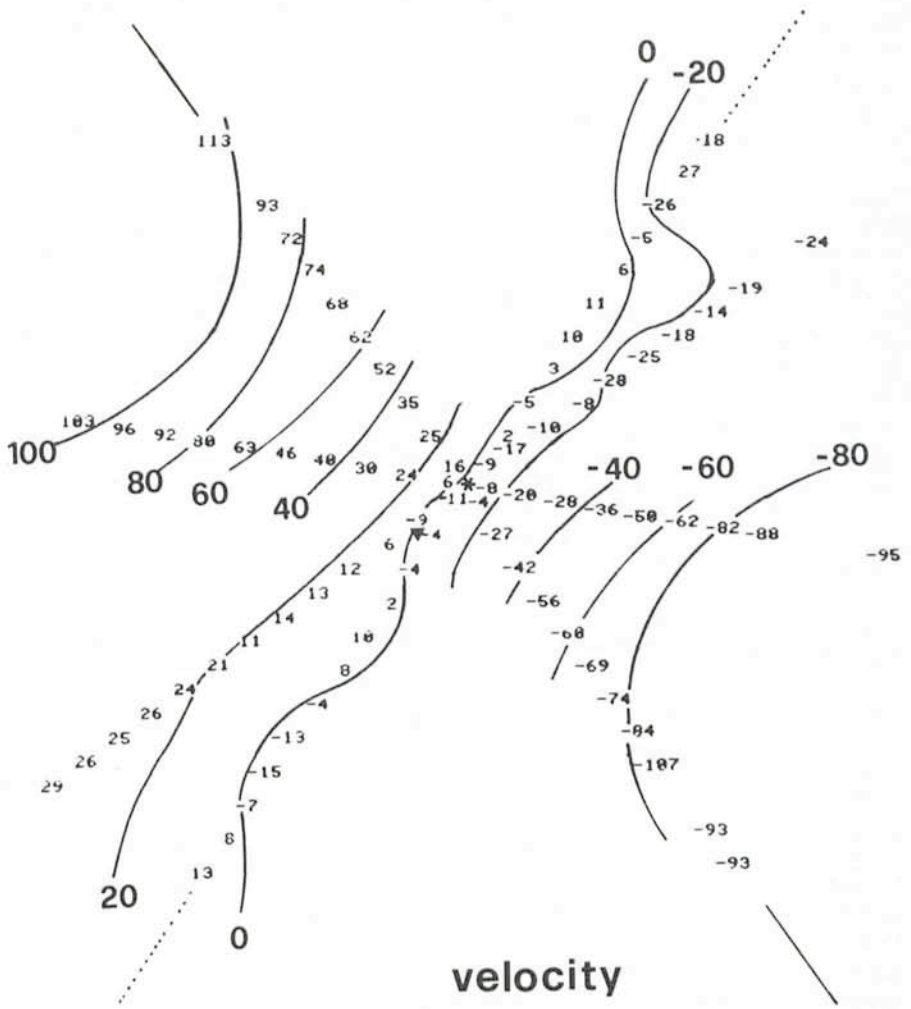

Figure 3: *The same as in Figure 1, but for the rotation curves. All the velocity values are scaled to the systemic velocity. A small triangle represents the approximate position of the symmetry point of the rotation curves.*

Discussion

The velocity dispersion field (Fig. 2) shows that σ is always decreasing outward, with the exception of the bar, where a narrow substructure of constant velocity dispersion (about 104 km/s) is seen. Since the bar is close to the zero velocity line, we can expect that the observed amplitude of the velocity dispersion is due to the sum of the stellar streamings along the bar. Contrary to the velocity map, the inner velocity dispersion field appears more symmetric around the nucleus instead of around the symmetry point of the velocities. If this effect is real, it indicates a quite complex velocity field.

The map of the velocity field shows two interesting features: First, the mean rotation at P.A. = 35° (near the major axis) and P.A. = 80° shows almost equal velocity values, an indication of elliptic orbits. An interpolation of the velocities observed outside the bar with a kinematical model of coplanar and elliptic orbits produces lines of equivelocity with a maximum velocity gradient at P.A. = 59°, 17° away from the direction of the disk major axis (see Fig. 3). Since at the maximum extent of the map (~ 40″ from the nucleus) the light of the bulge dominates, we must suppose that the bulge of NGC 6684 possesses elliptic orbits. Second, the line of zero velocity, aligned with the bar, follows a pattern symmetric with respect to a point not coincident with the galaxy nucleus. The position of this symmetry point, at about 4.5″ SE from the nucleus, is indicated in Figure 3 with a small triangle. Obviously this asymmetry is not due to obscillations of the velocity values because of the measuring errors. As said in the previous paragraph, a similar displacement from the nucleus has been observed also in the light distribution of the bar, but at NW, at the other side with respect to the symmetry point of the kinematics. This type of displacement between the bar, the optical nucleus and the centre of symmetry of the rotation curves is typical of Magellanic-type and late-type barred spirals, where it is connected with the presence of one or two points of equilibrium in the gravitational field. In barred S0s, kinematical asymmetries like that of NGC 6684 have been reported for NGC 936 (Kormendy 1983), but in a system where the bar isophotes do not show any asymmetry with respect to the nucleus of the galaxy. We can then suppose that the symmetry point observed in NGC 6684 could represent, with respect to the system bar + bulge, something like a Lagrangian point in the three-body problems of celestial mechanics. The shape

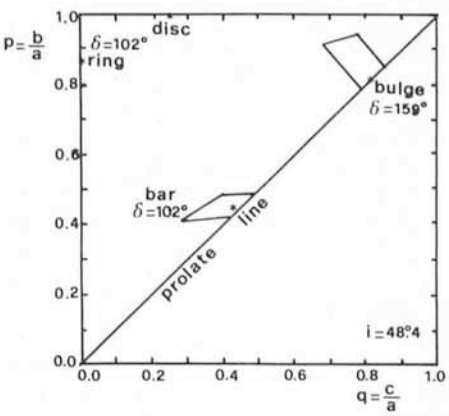

Figure 4: *Areas of possible solutions, in the plane c/a–b/a, for the intrinsic flattenings of each component of NGC 6684, as coming from our analysis of the geometry of the system. The asterisks indicate the exact solutions found or adopted. The angle on the plane of the galaxy is also indicated.*

of the isovelocity lines with $|v| \leq 20$ km/s is similar to that expected for the family of long axial orbits moving within the bars.

A geometrical model which can reproduce the shape of the isophotes has also been attempted, as described in the previous paragraph, by interpolation of the galaxy isophotes. From it results that (see Fig. 4 and Table 1): (1) The disk is probably oblate in shape. Despite the lack of kinematical information, its P.A. remains constant even if the flattening changes slightly, a feature typical of axisymmetric systems. (2) The bar is almost prolate, having similar axial ratios ($\underline{q} = 0.44$, $\underline{p} = 0.45$). (3) The ring cannot be circular, since it appears rounder than the disk and slightly misaligned. Its flattening and orientation are consistent with an elliptic structure aligned with the bar axis and with axial ratio 0.847. (4) According to the kinematics, the bulge could be triaxial. From the analysis of the possible solutions, excluding shapes as flat as the disk, we found a possible axial ratio of $\underline{q} = 0.817$, $\underline{p} = 0.824$, almost prolate, and elongated on the plane of the disk at 57° from the bar axis. But the roundness of its isophotes makes this last result quite uncertain.

A more complete analysis of the data is now in progress and will be compared with the data for the other SB0 systems included in the programme.

References

Bertola, F., Bettoni, D., Rusconi, L., Sedmak, G., 1984, *Astron. J.*, **89,** 356.

Corwin, H.G.Jr., Emerson, D., 1982, *Mon. Not. R. Astron. Soc.*, **200,** 621.

de Vaucouleurs, G., de Vaucouleurs, A., Corwin, H.G.Jr., 1976 (RC 2), *Second Reference Catalogue of Bright Galaxies* (Austin, University of Texas Press).

Galletta, G., 1983, *Astrophys. Space Sc.*, **92,** 335.

Kormendy, J., 1983, *Astrophys. J.*, **275,** 529.

Kormendy, J., 1984, *Astrophys. J.*, **286,** 132.

Sandage, A., Freeman, K.C., Stokes, N.R., 1970, *Astrophys. J.*, **160,** 831.

Williams, T.B., 1981, *Astrophys. J.*, **244,** 458.

IDS Spectroscopy of Planetary Nebulae

A. ACKER, Observatoire de Strasbourg, Centre de Données Stellaires, France

B. STENHOLM, Lund Observatory, Sweden

I. Introduction

From 1982 to 1984, Lundström and Stenholm conducted low-resolution spectroscopy of faint emission-line objects in the southern Milky Way (see Lundström, Stenholm, 1984). Their experience showed that the IDS is very efficient for spectroscopy of faint emission-line objects. They established that a mean exposure time of 10 minutes permits a clear classification of the observed objects, and a study of their most intense lines. Based on this study, we have undertaken, since 1984, a spectroscopic survey of the planetary nebulae. This study has been conducted with a double aim:

- realization of an atlas of calibrated spectra, within the framework of the forthcoming *Strasbourg-ESO Catalogue of Galactic Planetary Nebulae;*
- a statistical study of properties of the nebulae, in relation with problems of stellar evolution.

That means that most of the 1,500 objects known (1,100 in the southern sky) should be observed, essentially at La Silla, and at the Observatoire de Haute-Provence for the northern objects.

Status reports showing the earlier situation were given by Stenholm (1986), and Stenholm, Acker (1987).

II. The Observations and Reductions

In Table 1, some instrumental and observational parameters are summarized.

The apertures used are very small; most objects are, however, stellar-like, and this majority of objects is also the less observed part of the whole group. On the other hand, extended objects, particularly those of low surface brightness, are difficult to observe in this manner (10 minutes per object, in order to execute the programme during a reasonable period of time).

Table 2 presents the number of objects observed within each allocated observing run.

Here, we will report only about the observations done at La Silla. The status of the project is shown in the diagram in Figure 1. The reductions are carried out with the IHAP programme, working on the HP 1000 computer at La Silla, in Garching, at the Observatoire de Haute-Provence, and at the Institut de Physique du Globe de Strasbourg. Up to now, we have reduced all 723 spectra obtained at La Silla and measured line intensities for 220 of them.

III. Analysis of the Quality of the IDS Data

1. Reliability

To estimate the reliability of the whole system through different observing periods, we have compared the reduced fluxes obtained for independent spectra of spectrophotometric standard stars. We have obtained the following values of the spread $\Delta\varphi$ to the mean value φ of the flux calculated over the whole spectra:

star W 485 A (3 spectra)
$$<\Delta\varphi/\varphi> = 4{,}5\,\%$$
L TT 9239 (6 spectra)
$$<\Delta\varphi/\varphi> = 4{,}5\,\%$$
L 970–30 (6 spectra)
$$<\Delta\varphi/\varphi> = 7\ \ \%$$

2. Measurement of Blends

The measurement of line areas is done by using the *Multiple-Gaussian-Fit* procedure of IHAP for the blends of [N II]

Table 1: *Instrument Configurations*

	European Southern Observatory (ESO)	Observatoire Haute-Provence (OHP)
Telescope	1.52 m	1.93 m
Spectrograph	Boller & Chivens	CARELEC
Detector	IDS	CCD
Number of useful pixels	2053	511
Aperture	4 × 4″	2.5 × 4″
Approximate wavelength range	400–740 nm	385–740 nm
Dispersion	17 nm/mm	26 nm/mm
Approximate resolution	1 : nm	1 : nm
Normal exposure time	10 min	10 min